Investigation on the cavitating flow of biodiesel fuel within the nozzle passage according to the nozzle geometry

S. H. Park, B. W. Ryu, H. J. Kim, C. S. Lee*
Department of Mechanical Engineering
Hanyang University
17 Haengdang-dong, Sungdong-gu, Seoul, 133-791, Republic of Korea

Abstract

The high pressure fuel injection and complicated nozzle geometry caused an unstable flow field and the occurrence of cavitation by the dropping of the dynamic pressure at an inlet orifice. This cavitation inside nozzle orifice and the vortex flow in the sac volume affect the spray behavior and characteristics including the spray cone angle at nozzle exit. The purpose of this work is to investigate the internal flow characteristics using biodiesel fuel derived from soybean oil and the enlarged 2-dimensional nozzle, experimentally and numerically. In addition, it was studied the effect of the nozzle geometry such as a rectangular inlet shape, a tapered inlet shape, and another rectangular inlet orifice with different L/W (length / width) ratio on the cavitating flow characteristics of biodiesel fuel. A velocity distribution in a nozzle and a volume fraction of liquid / gas phase were calculated from the method of two-fluid model in FIRE code.

It was revealed that the length of cavitation get longer as increasing of the injection pressure after the occurrence of cavitation, and the cavitation grew along the nozzle orifice wall. Numerical results showed almost similar an inception point of caviation compared with experimental results. When the cavitation grew to near the nozzle exit, the flow velocity at the center of fuel flow increased. In addition, the spray cone angle of the injected fuel increased due to the increase of the relative velocity between the center and edge of the nozzle. In the case of the tapered inlet nozzle and the rectangular inlet nozzle with large L/W ratio, it needs a higher injection pressure to occur the nozzle cavitation compared to the rectangular inlet nozzle. At the tapered inlet nozzle, the volume fraction of liquid is smaller, and the flow velocity at the nozzle exit is higher than that of the rectangular inlet nozzle. The calculated cavitating flow from FIRE code was well agreed with the experimental cavitating flow.

Introduction

Nowadays, the injection pressure of diesel engine gets higher for the reduction of exhaust emissions through the fuel atomization of the injected spray and the improvement of the combustion performance. The high pressurization of diesel injection system and the complicated geometry of the injector nozzle essentially induced the cavitation phenomena. Practically, the nozzle cavitation which formed by the fast flow velocity and the big drop of static pressure near the inlet of nozzle orifice was emitted to the nozzle exit through the process of inception, growth, and collapse in a diesel injection system. Therefore, in the view point of the precise control of the injection system and the improvement of efficiency, studies on the inception and growth processes of cavitation inside the injector nozzle is indispensable. A lot of the experimental study on the caviation phenomena was actively progressed [1~3], and the caviation phenomena inside the real diesel injector nozzle was visualized by Liverani et al. [4], recently. In general, it is difficult to perform the experimental study for the cavitating flow inside the injector nozzle, because the diesel injector was very small, for example, nozzle diameter is about 150μm. Hence, the investigation using the enlarged visualization nozzle and the analytical study using various computational fluid dynamics (CFD) methods were performed by many researchers [5, 6]. There are two representative CFD approach methods. Homogeneous equilibrium model (HEM) [7] consider the nozzle flow as the mixture of liquid and vapor phase and solved the transport equations by using the mixture properties, such as density, viscosity and so on. On the other hand, two-fluid model [8] solved the transport equations weighed by volume fraction for each phases separately and compatibility condition that the summation of volume fraction was 1.

The purpose of this work is to investigate the internal flow characteristics using biodiesel fuel derived from soybean oil and the enlarged 2-dimensional nozzle, experimentally and numerically. In addition, it was studied the effect of the nozzle geometry on the cavitating flow characteristics of biodiesel fuel, such as a rectangular inlet shape, a tapered inlet shape, and another rectangular inlet orifice with different length/width (L/W) ratio. A velocity

*Corresponding author

distribution in a nozzle and a volume fraction of liquid/gas phase were calculated from the method of multi-fluid model in FIRE code.

Two-fluid model for calculation the cavitation phenomena

Two-fluid model was used to simulate the cavitating flow inside the nozzle in this study. In the two-fluid model, a set of the transport equations for each the phases was solved separately by addition of volume fraction and interfacial exchange term. Mass and momentum interactions between liquid and vapor phase of fuel were modeled and inserted into the source term of transport equations. The information of transport equations was minutely explained by von Berg et al. [8], and the source terms of mass and momentum exchange were presented since it included model constants influencing the calculation results. The linear cavitation model [8] linearlizing the Rayleigh-Plesset equation obtained from bubble dynamics. This model was used to calculate the mass exchange. The equation was described as follow.

$$\Gamma_{lv} = \frac{1}{C_{CR}} sign(\Delta P) 3.95 \frac{\rho_l}{\sqrt{\rho_v}} \left(N'''\right)^{\frac{1}{3}} \left(\alpha_v\right)^{\frac{2}{3}} \left|\Delta P\right|^{\frac{1}{2}} = -\Gamma_{vl} \quad (1)$$

where C_{CR} was condensation reduction factor which consider the condensation or evaporation of cavitation bubbles. ρ_l and ρ_v were liquid and vapor density respectively, α_v was volume fraction of vapor phase. In addition, N''' was number density of cavitation bubbles expressed by volume fraction phase and was calculated from following equation.

$$N''' = \begin{cases} N_0''' & \alpha_v \le 0.5 \\ 2\left(N_0''' - 1\right)\left(1-\alpha_v\right)+1 & \alpha_v > 0.5 \end{cases} \quad (2)$$

where N_0''' was the initial number density and it was defined as 10^{12}. ΔP was the effective pressure difference considering turbulent fluctuation as given by

$$\Delta P = P_{sat} - \left(P - C_E \frac{2}{3} \rho_l k_l \right) \quad (3)$$

where P_{sat} is the saturation pressure and was determined as 1,280 Pa which was the vapor pressure of biodiesel, C_E is the Egler factor, and k_l is the turbulent kinetic energy of liquid phase.

Momentum exchange was modeled including the drag and turbulent dispersion forces as given by

$$\mathbf{M_{lv}} = C_{TD} \rho_l k_l \nabla \alpha_v + C_D \frac{1}{8} \rho_l A_i''' \left|\mathbf{v_r}\right| \mathbf{v_r} = -\mathbf{M_{vl}} \quad (4)$$

where C_{TD} was the dispersion factor, A_i''' was the interfacial area density, and $\mathbf{v_r}$ was the relative velocity between liquid and vapor phase. C_D was the drag coefficient and was defined as following equation classified by Reynolds number of bubbles.

$$C_D = \begin{cases} \frac{192}{\mathrm{Re}_b}\left(1 + 0.10\,\mathrm{Re}_b^{0.75}\right) & \mathrm{Re}_b \le 1000 \\ 0.438 & \mathrm{Re}_b > 1000 \end{cases} \quad (5)$$

Calculation by using two-fluid model was performed from the commercial computational fluid dynamics (CFD) code-AVL FIRE.

Grid generation and calculation conditions

The calculation meshes for the three nozzle geometries were generated for studying the effect of the L/W ratio and inlet shape of test nozzles which influenced the cavitating flow inside the nozzle, as illustrated in Fig. 2. The grid was generated densely at the area where it is likely to occur the cavitation and unit cell size (0.5mm× 0.5mm) was the nearly same i.e., there are 12cells for the flow passage of the nozzle orifice, regardless of nozzle type. Calculation conditions for nozzle flow simulation were listed in Table 1. Boundary conditions for inlet and outlet were defined as the initial velocity and the pressure respectively. In order to identify the external flow, non-evaporating condition was used.

Experimental setup and procedure

In order to investigate the formation of cavitation in the nozzle and its effects on the outer injection characteristics, the experimental devices were manufactured and consisted as Fig. 1. Pressurized fuel for the needed flow rate conditions flows into the test nozzles through the fuel filter and flow rate meter (A109LMA, GPI). Used fuel circulated to original fuel tank using the fuel receiver and circulation pump (PW-200M, WILO). The inside nozzle flow

characteristics were visualized by ICCD (intensified charge couple device) camera (Dicam PRO, the Cooked Corp.) with the spot lamp using the shadow method. The digital camera (D100, Nikon) was used to capture the outer flow patterns of biodiesel fuel. In this work, three test nozzles, which were made from the acrylic acid resin, were used for observing and analyzing the caviation in the nozzle orifice and its effects on the flow patterns. Effect of the L/D (length/diameter) ratio was analyzed using two test nozzles with the rectangular inlet shape (L/D = 1.5 and 3) as shown in Fig. 2(a) and (b). In addition, the effect of the nozzle inlet shape on the formation characteristics of cavitation was analyzed using other two nozzles as illustrated in Fig. 2 (a) and (c). Detailed specifications of test nozzles can be seen in Fig. 2. In order to examine the internal and external flow characteristics and the effect of cavitation on the fuel flow patterns, experimental flow rates were controlled from 1 L/min to 5 L/min, and the test fuel were used SME (soybean methyl ester). The kinematic viscosity and density of SME are 4.1cSt (313.2K) and 884g/L (288.7K), respectively.

Results and Discussion

Discharge coefficient for the injection pressure and the dimensionless number characteristics of test nozzles using biodiesel fuel were shown in Fig. 3. In this investigation, the flow characteristics of cavitating flow were analyzed in terms of following dimensionless numbers such as Reynolds number ($\mathrm{Re} = \rho VW / \mu$), the cavitation number($K = 2(P_b - P_v) / \rho V^2$), and Weber number ($We = \rho V^2 W / \sigma$). In addition, the discharge coefficient was considered for analyzing the cavitating flow of the injector nozzle. The discharge coefficient is the ratio of the ideal flow rate which was derived by the continuous equation and Bernoulli's equation to the actual flow rate measured from the flow rate meter. As illustrated in Fig. 3(a), the discharge coefficient of Nozzle A and B is a similar value in the turbulent flow and cavitating flow regions. On the other hand, Nozzle C has a higher C_d than other test nozzles, because the Nozzle C with tapered inlet shape has a low flow resistance compared to other nozzles. In addition, the discharge coefficient of each nozzle after the occurrence of the hydraulic flip suddenly decreased, because the effective flow area reduced by the hydraulic flip phenomena. As shown in Fig. 3(b), Re and We exponentially decreased with the increase of the K, and the variation pattern of three test nozzles have coincident each other.

In three different nozzles, the variation process of the spray angle according to the inception, growth, and collapse of cavitation was illustrated in Fig. 4. Although there are the differences of the degree, the spray angle increase as the turbulent flow transferred the cavitating flow. It is guessed that the collapsed energy of the cavitation and the injection pressure for the formation of cavitation is the causes of the increase of the spray angle. In case of the small L/W ratio nozzle (Nozzle A), the increment of the spray angle is larger than the large L/W ratio nozzle (Nozzle B). It is postulated that the stored energy inside the cavitation dissipated in the nozzle orifice according to the extension of the nozzle orifice, as the L/W ratio becomes large. In addition, in the case of the nozzle orifice with tapered inlet shape, the cavitation phenomena little affect to the spray angle, because the occurrence level of cavitation is very small.

Figure 5 shows the comparison of the inception of caviation and cavitating flow between experimental and numerical results. The inception and development of cavitation flow were confirmed through the variation of the liquid volume fraction in the numerical results obtained from FIRE code. The low volume fraction means an active formation and development of cavitation phenomena. As illustrated in Fig. 5(a) and (b), the numerical results (right-side of the image) described similar patterns to the experimental results at three test nozzle geometries. However, the injection pressures for the occurrence and growth of cavitation were somewhat different in the comparison of the experimental and numerical results. It can be guessed that the difference was generated from the in-homogeneity of test fuel and the frictions from the roughness of nozzle orifice wall that the numerical code did not consider.

In the grown cavitation region of the calculation results, the distribution of the liquid velocity profile at various nozzle orifice positions was represented in Fig. 6. As the flow reached the inlet of the nozzle orifice, the velocity inside the nozzle increased due to the contraction of orifice inlet areas in three test nozzles. When the caviation occurred at the nozzle wall, the direction of liquid flow was headed to the center, because of the rapid reduction of pressure. In addition, the two wing peaks appeared close to the boundary of cavitation region at the inlet of nozzle orifice [9]. In the cavitation regions, the flow velocity at the center of orifice was highest at the cross sectional area, because the interaction between the vapor and liquid phase little affects the flow velocity of the orifice center. At the nozzle exit, the flow velocity was slightly decreased due to the extension of the flow area and different velocity around the nozzle wall. On the other hand, the flow velocity at the starting position of the cavitation and the injection pressure for the inception of cavitation in the case of Nozzle C were somewhat higher than those of other nozzle geometries. It can be guessed that the tapered inlet geometry relieved the resistance by the change of the flow direction, and simultaneously, restrained the occurrence of cavitation.

Conclusions

This work dealt with the experimental and numerical study on the inception and growth of the caivating flow inside the nozzle orifice. Based on the results and discussion, the conclusions of this study were arranged as follows.

1. The discharge coefficient was affected by the orifice inlet shape, not the length to width of the nozzle orifice. Therefore, Nozzle C with the tapered inlet shape has a highest discharge coefficient, because the tapered inlet shape relaxed the flow resistance. In addition, the variation patterns of dimensionless number, such as Reynolds number, Weber number, and cavitation number are almost consistent at the three test nozzles.
2. The spray cone angle at the nozzle exit increased in the region of cavitating flow, and then it suddenly decreased at the hydraulic flip region, because the collapsed energy of cavitation at the nozzle exit affects the spray behavior. On the other hand, the cavitation phenomena little affects to the spray cone angle in the nozzle orifice with tapered inlet shape, because the occurrence intensity of cavitation is very low.
3. The numerical results using the two-fluid model implemented into FIRE code well described the experimental results. However, the occurrence conditions for the inception and growth of cavitation were somewhat different, because the numerical code do not sufficiently reflected the roughness of the nozzle orifice and in-homogeneity of test fuel.
4. The sudden contraction of the flow area at the orifice inlet induced the increase of the flow velocity and the decrease of the dynamic pressure of flow fluid. These phenomena caused the occurrence of the cavitation. In the cavitation regions, the flow velocity at the center of orifice was highest at the cross sectional area, because the interaction between the vapor and liquid phases little affects the flow velocity of the orifice center.

Nomenclature

A_i'''	the interfacial area density
C_{CR}	the condensation reduction factor
C_D	the drag coefficient
C_E	the Egler factor
$\mathbf{M}_{lv}$, $\mathbf{M}_{vl}$	the momentum exchange
N'''	the number density of cavitation bubbles
P	Pressure
Re_b	Reynolds number of bubbles
$\boldsymbol{v_r}$	the relative velocity between liquid and vapor phase
α_v	the volume fraction of vapor phase
ρ	density
k	the turbulent kinetic energy of liquid phase
Γ_{lv}, Γ_{vl}	the mass exchange

Subscript

0	initial
sat	saturation
l	liquid
v	vapor

References

1. Li, H. and Collicott, S. H., *Atomization and Sprays* 16:875-886 (2006)
2. Arcoumanis, C., Flora, H., Gavaises, M., Kampanis, N., and Horrocks, R., *International Congress and Exposition(SAE-International)*, Detroit, USA, April, 1999, SAE1999-01-0524
3. Sou, A., Hosokawa, S., and Tomiyama, A., *International Journal of Heat and Mass Transfer* 50:3575-3585 (2007).
4. Liverani, L., Arcoumanis, C., Yanagihara, H., Sakata, I., and Omae, K., *the Seventh international Conference on Modeling and Diagnostics for Advanced Engine Systems*, Sapporo, Japan, July, 2008, pp. 454-460.
5. Park, S. H., Suh, H. K, and Lee, C. S., *Energy & Fuels* 22:605-613 (2008).
6. Payri, R., Margot, X., and Salvador, F. J., *SAE 2002 World Congress*, Detroit, USA, March, 2002, SAE2002-01-0215.
7. Ning, W., Reitz, R. D., Diwakar, R., and Lippert, A. M., *SAE 2008 World Congress*, Detroit, USA, April, 2008, SAE2008-01-0936.
8. von Berg, E., Edelbauer, W., Alajbegovic, A., Tatschl, R., Volmajer, M., Kegl, B., and Ganippa, L. C., *Journal of Engineering for Gas Turbines and Power* 127:897-908 (2005)

9. Soteriou, C., Andrews, R., and Smith, M., *SAE International Spring Fuels & Lubrications Meeting & Exposition*, Michigan, May, 1999, SAE1999-01-1486.

Table 1. Experimental and calculated conditions for the nozzle flow

Experimental and calculated conditions	Injection pressure (MPa) Ambient pressure (MPa) Ambient temperature (K)	0.13 ~ 0.45 0.1 293.15
Test nozzle	Nozzle A(Rectangular inlet, L/W=1.5) Nozzle B(Rectangular inlet, L/W=3.0) Nozzle C(Tapered inlet, L/W =1.5)	
Test fuel	Biodiesel fuel derived from the soybean oil	

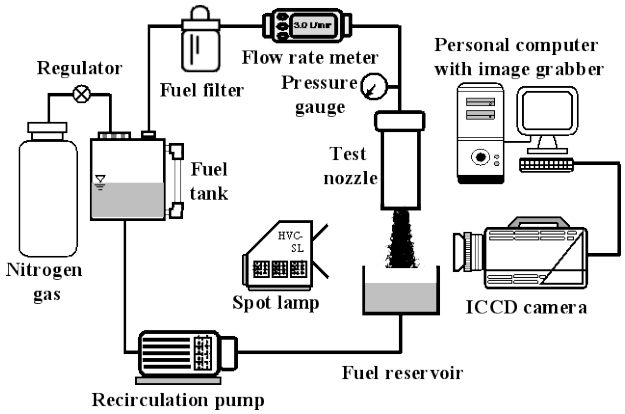

Figure 1. Schematic of the experimental device for visualization of cavitating flow inside the nozzle

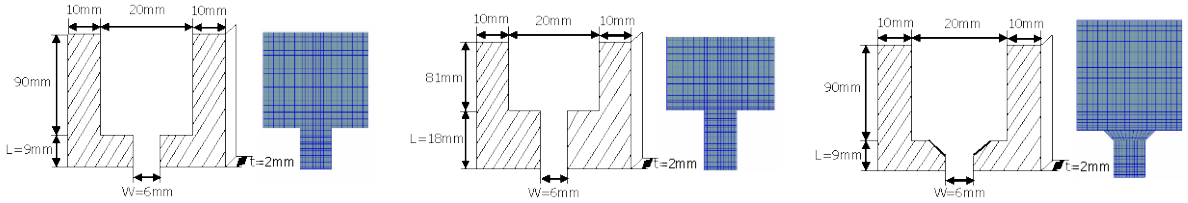

(a) Nozzle A (L/W = 1.5) (b) Nozzle B (L/W = 3) (c) Nozzle C (tapered inlet shape)

Figure 2. Schematics of three test nozzles and computational grids

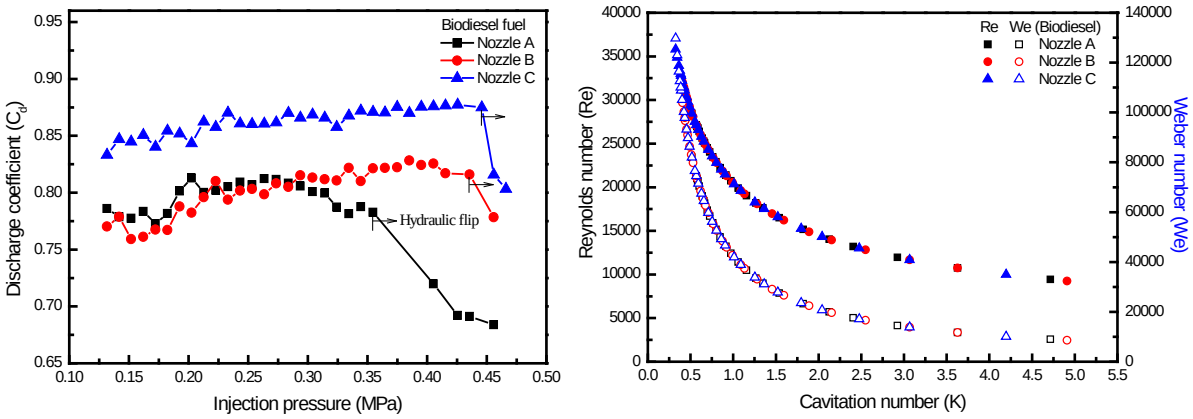

(a) Discharge coefficient for the injection pressure (b) Dimensionless number characteristics

Figure 3. Comparison of the discharge coefficient for the injection pressure and the dimensionless number characteristics of test nozzles

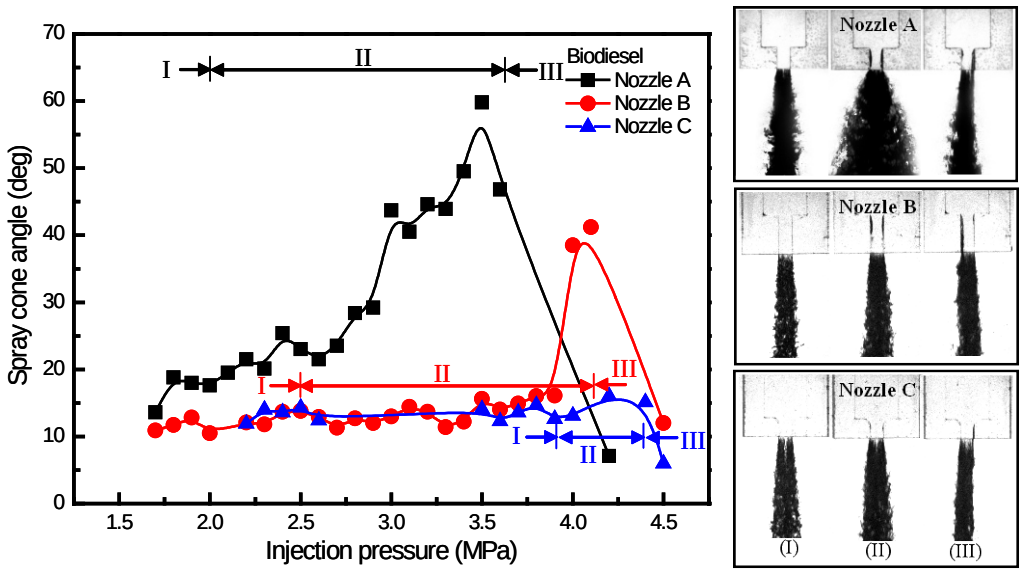

Figure 4. Characteristics of the spray angle according to the growth process of cavitation and the external flow pattern according to the internal flow of test nozzles (I: turbulent flow, II: cavitating flow, III: hydraulic flip)

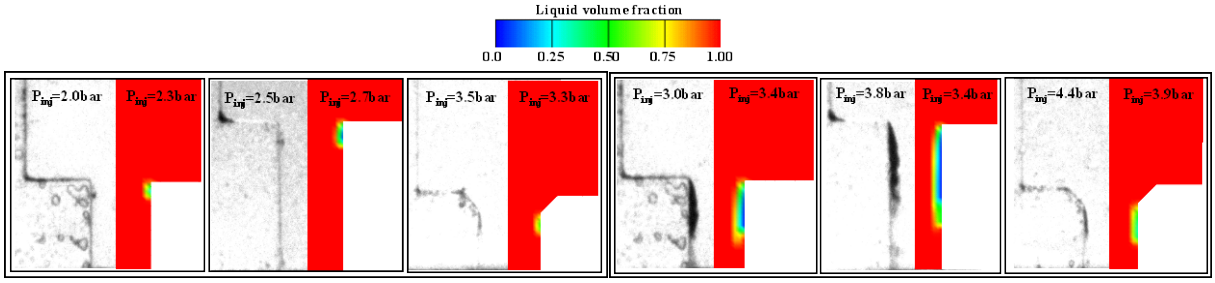

(a) Inception of cavitation (b) Cavitating flow

Figure 5. Comparison of internal flow pattern between experimental and numerical images

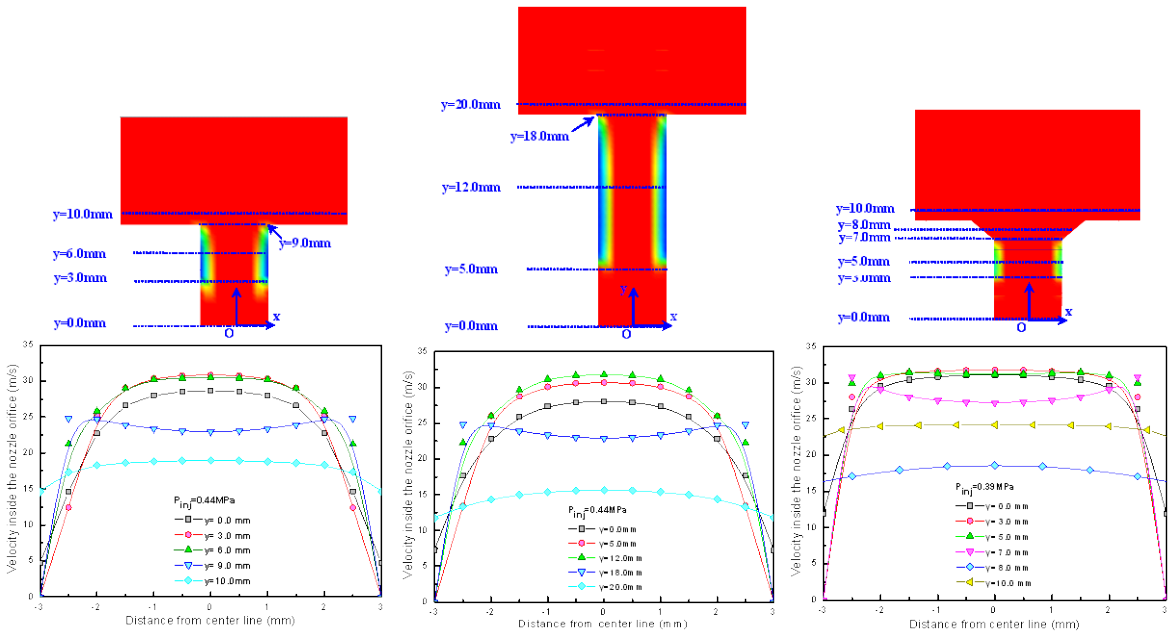

Figure 6. Distribution of the liquid velocity profile at various orifice positions